Int. Journal of Refractory Metals and Hard Materials 54 (2016) 260–269

Contents lists available at ScienceDirect

Int. Journal of Refractory Metals and Hard Materials

journal homepage: www.elsevier.com/locate/IJRMHM

Mechanical wear of different crystallographic orientations for single abrasive diamond scratching on Ta12W

Haiyong Wu [a,b], Hui Huang [a,*], Feng Jiang [a], Xipeng Xu [a]

[a] Institute of Manufacturing Engineering, Huaqiao University, Xiamen, 361021 Fujian Province, PR China
[b] Department of Mechanical and Automation Engineering, Zhangzhou Institute of Technology, Zhangzhou, 363000 Fujian Province, PR China

A R T I C L E   I N F O

Article history:
Received 9 April 2015
Received in revised form 20 July 2015
Accepted 28 July 2015
Available online 1 August 2015

Keywords:
Diamond
Scratch testing
Wear
Crystallographic orientation

A B S T R A C T

Mechanical wear is one of the dominant modes in abrasive machining. Single crystal diamond (SCD) mechanical wear characteristics with different crystallographic orientations (SCD_{100} and SCD_{111}) during scratching on Ta12W were systematically investigated. The wear mechanism involved in the scratching was explored. The scanning electron microscope examination of the worn SCD and the analysis of the wear volume, scratching force and acoustic emission signals involved in the scratching process indicated that the mechanical wear progression of two SCD grits is obviously different. A standard scratch tester experiment with a conical indenter was also carried out. It was found that the scratching force ratio for a SCD_{100} grit was similar with the friction coefficient in the standard scratch tester, which was higher than the case for a SCD_{111} grit. The wear resistance of the SCD_{111} grit is greater than the SCD_{100} grit in a normal wear situation. However, the SCD_{100} grit has a much longer scratching life than the SCD_{111} grit. Different stress and crystallographic orientations result in different cleavage fracture modes.

1. Introduction

Single crystal diamond (SCD) is widely used in machining metals, brittle materials and other hard materials [1,2] because it possesses excellent mechanical properties such as extreme hardness, thermal conductivity, and corrosion and wear resistance. Diamond tool wear is an influential factor in the machining process. Previous studies have demonstrated that the wear morphology of the abrasive diamond during sawing and grinding process mainly includes five modes such as fresh, rubdown, micro-fractured, macro-fractured and pulled out although there are various geometries, protrusions and stochastic distributions of diamond abrasives [3,4]. Almost all the modes of diamond abrasive wear can be included into three classifications: mechanical, chemical, and thermal wear [5]. The mechanical wear of a diamond abrasive grit plays an important role in the machining process, and it can be described as the deformation and fracture generated by mechanically induced strains and stresses.

Much attention has been given to the influence of crystallographic characteristics on the mechanical wear of SCD grits during SCD precision and ultra-precision machining processes [6–8]. The SCD turning tool with different crystallographic orientations such as flank face and rake face exhibits variations in wear progression and characteristics during actual machining operations [9,10]. However, to date, there are few studies from the literature about the effects of crystallographic orientation on the mechanical wear mechanism of the abrasive SCD grits in the grinding/sawing process.

This paper attempts to present and illustrate the influence of crystallographic orientation on the abrasive SCD mechanical wear characteristics during single SCD grit scratching. The common abrasive SCD grits with different crystallographic orientations were employed in the scratching process. The standard scratch tester experiment with a conical indenter was also carried out [11–13]. The morphology of the SCD wear characteristics and the wear volume were tracked. The scratching forces and acoustic emission (AE) signals were measured to analyze the mechanical wear progression of the single abrasive SCD grit.

2. Experimental procedure

In this experiment, common abrasive SCD grits with particle sizes of 0.6–0.85 mm (Element Six SDB 1125 20/30 mesh) such as those shown in Fig. 1 were employed to fabricate single SCD tools. The SCD grit is cuboctahedral and enclosed by two different crystallography geometrical shapes: square and triangular. The square and triangular crystal planes are {100} plane and {111} plane respectively. Two different crystal planes of SCD abrasive grits were oriented towards the workpiece in the grit–workpiece contact area respectively as shown in Fig. 2(a,c). The two types of crystallographic orientations of SCD abrasive grits were denoted as SCD_{100} and SCD_{111}. The crystal direction might have an effect on the mechanical wear of the SCD grits [14]. To focus on the effect of crystallographic orientation on the mechanical wear of a SCD

* Corresponding author.
E-mail addresses: haiyongwu@hotmail.com (H. Wu), huanghuihh@hotmail.com (H. Huang).

http://dx.doi.org/10.1016/j.ijrmhm.2015.07.038
0263-4368/

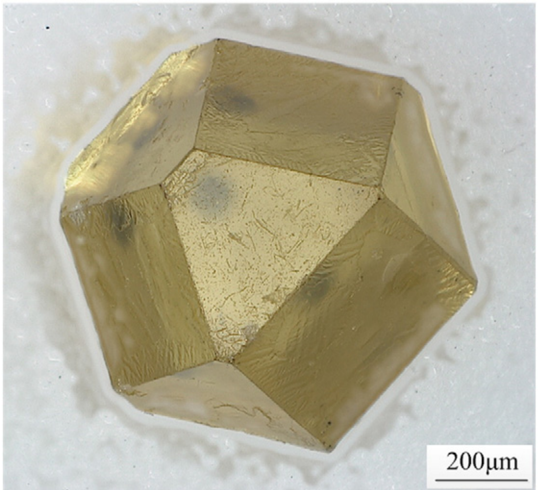

Fig. 1. The cub-octahedral abrasive SCD grit is employed in the experiment.

grit, the abrasive SCD grits scratch on the workpiece with different crystallographic orientations in the same crystal direction. The scratching direction was parallel to the <110> crystal direction of the two SCD grits. The SEM images from top view of the SCD grits are shown in Fig. 2(b,d).

To investigate the mechanical wear of the abrasive SCD grits during the scratching process, the workpiece has to meet the conditions including: (1) excellent wear resistance, (2) high temperature resistance, (3) without chemical reaction with the SCD grits during the scratching. The alloy Ta12W mainly contains the nonferrous metallic element of tantalum and tungsten, its material properties are shown in Table 1. From Table 1, it can be observed that the Ta12W has high hardness and melting temperature. All of these characteristics just meet the requirements above. Therefore, the Ta12W is selected as the workpiece material in the scratching experiments.

The SCD grit scratching test was performed by a CNC surface grinding machine (Planomat HP 408). The scratching test setup is shown in Fig. 3. The workpiece material was stuck on the clamp mounted on the dynamometer. A single abrasive SCD grit was brazed on stainless steel blind nuts with Ni–Cr–B–Si alloy. The stainless steel blind nuts were mounted to the dummy wheel. The scratching speed v_s = 20 m/s, workpiece feed rate v_f = 0.01 m/s, and depth of cut a_p = 10 μm. The scratches on the workpiece surface overlapped and formed into a groove.

The AE sensor (Physical Acoustics Micro-II type) was mounted near the workpiece to acquire the AE signals during the scratching tests. The AE sampling frequency was 10 MHz, the sampling bandwidth was 1 k–1 MHz, the sampling length was 15 k, the threshold value was 55 dB, and the pregain was 20 dB. The scratching force was measured by the dynamometer (Kistler Type-9257B), and the dynamometer was in conjunction with a Kistler charge amplifier and DEWE 2010 digital recorder. The sampling frequency was 50 kHz.

SEM (FEI Phenom prox) images of the SCD grits were inspected after a constant distance scratching each time. The wear volume of the SCD grits and the workpiece material removal volume were metrologically measured by a confocal laser scanning microscope (Carl Zeiss LSM700), and the SCD grits were mounted on a special fixture to keep the same field of view under the laser scanning microscope.

The standard scratch tester was carried out on a multifunctional surface property tester (MFT-4000). The conical diamond tools used in the standard scratch tester had an included angle of 120° with a 0.2 mm round radius. The linear speed of the conical diamond was kept constant at 4 mm/min. The scratch load increased from 0 to 100 N evenly in the

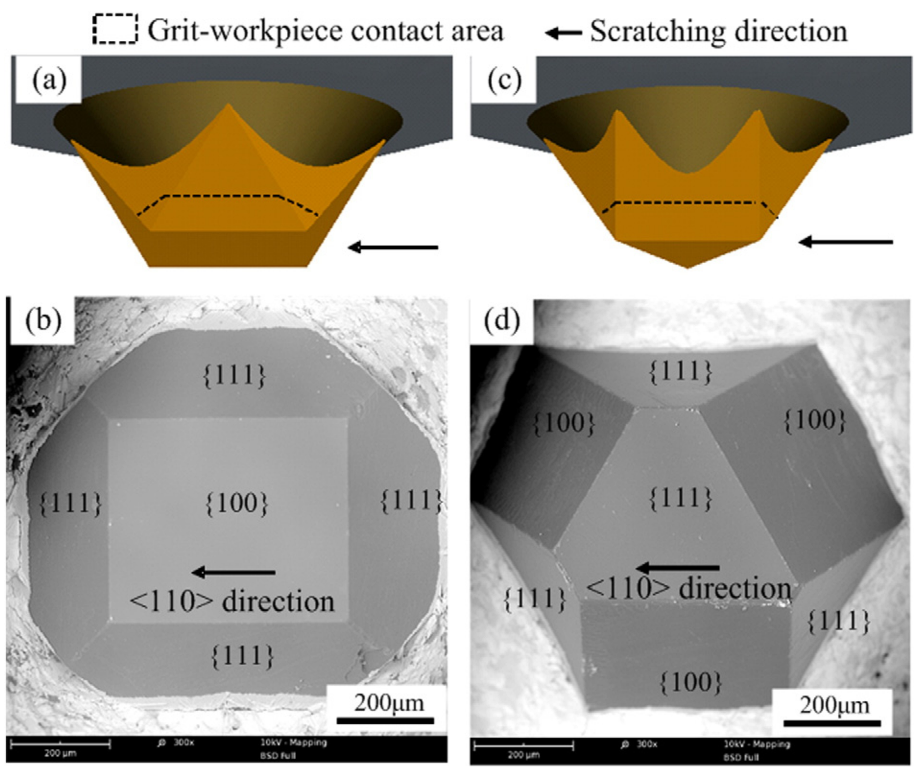

Fig. 2. Conceptual graphs from the front view and SEM images from the top view of the SCD_{100} grit (a, b) and SCD_{111} grit (c, d).